Fabrication of Micro-Grooves in Silicon Carbide Using Femtosecond Laser Irradiation and Acid Etching *

KHUAT Vanthanh[1,2], MA Yun-Can(马云灿)[1], SI Jin-Hai(司金海)[1**], CHEN Tao(陈涛)[1],
CHEN Feng(陈烽)[1], HOU Xun(侯洵)[1]

[1]Key Laboratory for Physical Electronics and Devices of the Ministry of Education and Shaanxi Key Lab of
Information Photonic Technique, School of Electronics and information Engineering,
Xi'an Jiaotong University, Xi'an 710049
[2]Le Quy Don Technical University, Hanoi 7EN-248, Vietnam

A simple method using an 800-nm femtosecond laser and chemical selective etching is developed for fabrication of high-aspect-ratio grooves in silicon carbide. Micro grooves with an aspect ratio of approximately 40 are obtained. The morphology and chemical compositions of the grooves are analyzed using a scanning electronic microscope equipped with an energy dispersive x-ray spectroscopy. The formation mechanism of SiC grooves is attributed to the chemical reactions of the laser induced structural changes with a mixed solution of hydrofluoric acid and nitric acid. In addition, the effects of laser irradiation parameters on the aspect ratio of the grooves are investigated.

Due to its small size, excellent performance, low cost and high volume production, microelectromechanical systems (MEMSs) have attracted increasing attention of researchers. Silicon-based MEMS devices have been well developed. These devices are generally limited in electronic devices performance to below 250℃, and in mechanical device performance to below 600℃. They are not suitable working in the corrosive environment since Si could be easily etched by acid solutions. Silicon carbide (SiC) is a promising candidate for MEMS applications in harsh environments due to its outstanding physical and chemical properties.[1−6] SiC-based devices are capable of working in harsh temperatures, wear, chemical, and radiated environments.[7−9] Commonly, the main method used for drilling and patterning SiC is the dry etching technique.[10−14] However, the low processing rate, the necessity of having micro-masks in the etch field, and the complexity of the processing procedure are the main drawbacks of this technique. Recently, an ultrafast laser has been proposed as an effective tool for micromachining SiC. Laser micromachining has several prominent advantages over conventional methods, such as noncontact processing, fast removal rates and being independent on etch masks.[15−20] Additionally, laser direct writing is capable of fabricating three-dimensional micromechanical devices since the samples can be mounted onto a programmable positioning stage. Fabricating grooves in SiC has attracted increasing interest of researchers due to their potential applications in microelectronics, optoelectronics, microchemical systems, microelectromechanical systems (MEMS), microbiology and so on. Plenty of studies have been focused on the ablation threshold and morphology of SiC surface structures processed with an 800-nm femtosecond laser.[21−25] However, little research has been conducted on the fabrication of high-aspect-ratio grooves in SiC with an 800-nm femtosecond laser. Due to the fact that SiC is transpar-

ent to the 800-nm light wave, an 800-nm femtosecond laser is capable of inducing structural changes with a high aspect ratio, which could be removed with the proper etching technique. Therefore, we predict that the combination of an 800-nm femtosecond laser with chemical etching could be ideal for fabricating high-aspect-ratio grooves in SiC. However, there has been no report on using this method to fabricate grooves in SiC.

In this Letter, we propose a simple method of fabricating high-aspect-ratio grooves in SiC, in which the femtosecond laser irradiation and chemical selective etching with a mixed solution of hydrofluoric acid (HF) and nitric acid (HNO_3) are combined. Firstly, the laser induced structural change (LISC) zones are produced with irradiation of an 800-nm femtosecond laser. Then, mixed solution of HF and HNO_3 is used to remove the LISC zones, forming the grooves in SiC. Subsequently, a scanning electronic microscope (SEM) equipped with an energy dispersive x-ray spectroscope (EDS) is employed to analyze the morphology and chemical compositions of the LISC and the SiC grooves, respectively. Furthermore, we systematically investigate the dependencies of the aspect ratio (AR) of the grooves on the numerical aperture (NA) of the microscope objective lens, the laser average power P and the laser scanning velocity v, respectively.

The experimental setup consists of a femtosecond laser source, an attenuator, a neutral density filter, a mechanical shutter, an xyz movable stage, a computer and a CCD camera. The laser used was an amplified Ti:sapphire femtosecond laser system (Coherent Inc., USA) with pulse duration of 150 fs, wavelength of 800 nm, and repetition rate of 1 kHz. An attenuator provided a convenient way to adjust the laser energy, while a mechanical shutter was employed to control the access laser beam. A movable stage, on which the SiC sample could be mounted, controlled by the computer program, allows us to fabricate on the pattern

**Corresponding author. Email: jinhaisi@mail.xjtu.edu.cn

with high precision. The CCD camera was connected to a computer for clear online observation in SiC pattern surface during the fabricating process.

In our experiments, the 6H-SiC pattern with a thickness of 300 μm was used. Firstly, it was cleaned in acetone and de-ionized water with an ultrasonic field for 10 min, respectively. Then it was mounted on the movable stage. The laser beam was focused onto the pattern via an optical microscope objective lens. During the fabrication, the surface of the SiC pattern could be seen either via an optical microscope or on the computer screen connected to the CCD camera. It should be noted that the scanning direction was set parallel to the y-axis, which was parallel to the polarization direction of the incident laser.
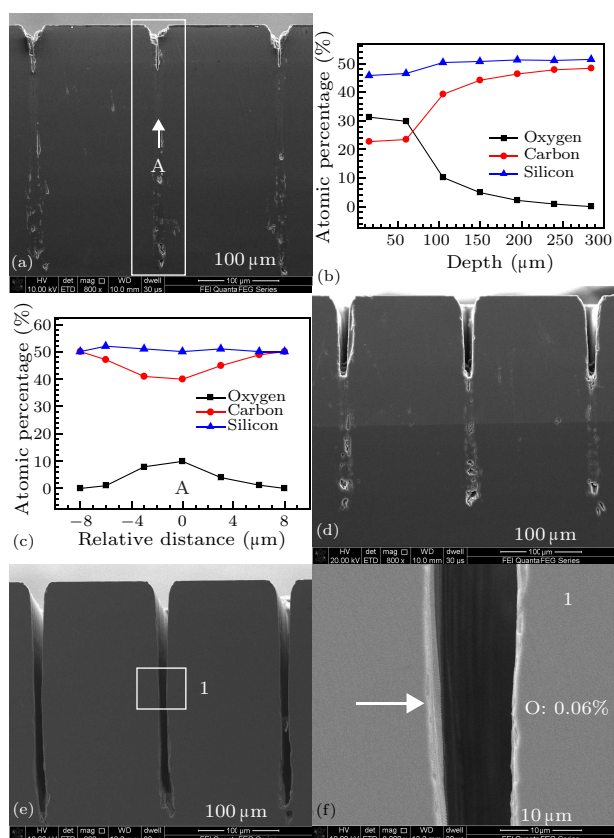
Fig. 1. SEM images morphology of SiC grooves. (a) The LISC (as marked with white box). (b) Atomic percentage along the longitudinal direction of the LISC. (c) Atomic percentage along the horizontal direction of the LISC at 105 μm depth. (d) After etching with HF. (e) After etching with mixed solution of HF and HNO$_3$. (f) The middle part.

After the laser irradiation, we polished the SiC pattern with waterproof abrasive papers to a random position to observe the LISC from the cross section. The pattern is then cleaned consecutively with acetone and de-ionized water for 10 min before being selectively etched with a mixed solution of 40wt% HF and 60wt% HNO$_3$ for 10 min. SEM equipped with EDS was employed to study the morphology and chemical composition of SiC grooves before and after etching.

Figure 1 shows the morphologies of the LISC and the chemical etching induced SiC grooves. The grooves were fabricated in ambient air. A 10× micro-

scope objective with NA of 0.3 was employed to focus the laser onto the surface of the SiC sample. The laser average power and scanning velocity were set at 30 mW and 5 μm/s. After being irradiated with an 800-nm femtosecond laser, the sample was polished to a random position of the grooves. LISC was induced at the irradiated zones in the direction of the femtosecond laser transmission. The cross section of the LISC is shown in Fig. 1(a). Concerning the LISC, there has been no report on the 800-nm femtosecond laser induced such as microstructures in the interior of SiC. We attribute the formation of LISC to the change in structure of SiC caused by the interaction of the femtosecond laser and the material. For an ultra-short laser pulse, multiphoton absorption is considerably strong. Although 800-nm photons cannot meet the 6H-SiC band gap energy (3.1 eV) requirements, bond breaking is induced by multiphoton absorption associated with the extreme intensity. Laser induced heating and stress could generate dangling bonds in original hexagonal crystal structure of 6H-SiC. These dangling bonds make the LISC chemically and physically less stable as compared to the original SiC. The incorporation of oxygen atoms (O) in the material could be attributed to the trapping effect of dangling bond.[26]
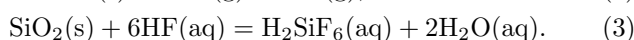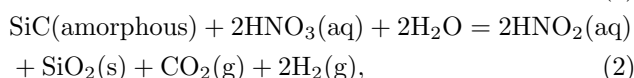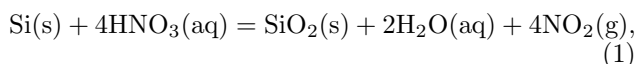
The EDS results illustrated in Fig. 1(b) show the change in the structure of LISC. The ratio of carbon and silicon (C/Si) experiences a sharp change along the LISC depth. Near the surface, it is much smaller than 1, and with the increase of LISC depth the C/Si ratio increases until reaching 1 as shown in Fig. 1(b). This is due to the redistribution of Si and C caused by the non-equilibrium condition of rapid heating and cooling in laser treatment. Meanwhile, foreign oxygen species was incorporated in the interior of the SiC substrates. Contents of O species decrease with the increase of the LISC depth. This is due to the fact that the concentration of the femtosecond laser induced dangling bonds decreases with the decrease of laser intensity. Number of the dangling bonds decreases along the laser transmission direction in the longitudinal direction. Therefore, the ability to accommodate foreign species of SiC decreases, resulting in the decrease of the atomic percentage of the incorporated O species with the increase of LISC depth.

Figure 1(c) shows the change in the structure of LISC in the horizontal direction at the depth of 105 μm (marked with point A in Fig. 1(a)). It is obvious that the content of O is maximal at the center of the LISC and becomes smaller at the edge. At the same time, from the center to the edge of the LISC, the ratio C/Si increases. This is due to the fact that the laser was a Gaussian beam of which the fluence is strong at the center and becomes weaker at the edge of the beam.

Figure 1(d) shows the LISC after being etched with HF for 1 h. It could be seen that only the part near the surface of the LISC was removed. We speculate that, near the surface, O species existed in the LISC in the form of silicon oxide (SiO$_x$) and this part was removed due to the reaction of HF and SiO$_x$. While in the remaining part of the LISC, there was only a

change in structure of SiC and it could not be etched using the HF solution.

Figure 1(e) shows the grooves produced by the laser treatment and having been etched with a mixed solution of HF and HNO_3 for 10 min. The pattern was again polished to a random position along the groove to see the cross section of the groove. Due to the chemical reactions of mixed solution of HF and HNO_3 with LISC, which is possibly composed of SiO_x, pure Si and chemically non-stable form of SiC, the LISCs were completely removed, forming grooves in SiC. The related chemical processes are shown as follows:[27,28]

$$Si(s) + 4HNO_3(aq) = SiO_2(s) + 2H_2O(aq) + 4NO_2(g), \tag{1}$$

$$SiC(amorphous) + 2HNO_3(aq) + 2H_2O = 2HNO_2(aq)$$
$$+ SiO_2(s) + CO_2(g) + 2H_2(g), \tag{2}$$

$$SiO_2(s) + 6HF(aq) = H_2SiF_6(aq) + 2H_2O(aq). \tag{3}$$

In the above reaction progresses, HNO_3 acts as the oxidizing agent, and HF removes the SiO_x generated from the laser treatment process, Eqs. (1) and (2). It should be noted that only the LISC reacted with the acid solution, while the surrounding zones remained unchanged. This indicates the high selectivity of the method. After being etched, the wafers were rinsed in the ultrasonic cleaner with acetone and de-ionized water for 10 min to eliminate the remaining reactants HF and HNO_3 and the by-product fluosilicic acid (H_2SiF_6), respectively. It can be seen from Figs. 1(e) and 1(f) that the sidewalls of the grooves are very smooth. Meanwhile, the atomic percentages of O in the surrounding area of the grooves were in the range of the measurement deviation of the EDS analysis, which could be ignored. In the following, we are going to discuss the effects of the femtosecond laser irradiation parameters on AR of the grooves.

To investigate the effects of the numerical aperture (NA) on the quality of the grooves, five microscopes of different NAs have been employed to fabricate the grooves while the scanning velocity and the laser power were 5 μm/s and 30 mW, respectively. Figure 2 shows the dependency of AR on NA. The inset shows the representative of the groove produced as NA is 0.3. It is obvious that AR decreases as NA increases. For example, with NA of 0.3 AR is 37; while it is 5 as NA is 0.45; and with NA of 0.9 AR is 1. Moreover, as NA increases, the cross-sectional shape of the grooves changes from a rectangular shape to an ellipse, while the entrance width decreases. This is due to the fact that NA characterizes the focus capacity of the lens to the incident laser beam. That is, larger NA means smaller laser spot sizes at the focal plane and shallower focal depth. Therefore, with the same set of laser cutting parameters, the entrance width and depth of the LISC decrease with the increase of NA. Simultaneously, there exists competition between the self-focusing due to the nonlinear Kerr effect and the self-defocusing resulted from the thermal accumulation in femtosecond laser irradiation.[29] As the laser beam is loosely focused, the self-defocusing is dominant. The cross-sectional shapes of the photoinduced LISC are multiple slim ellipses. As the laser beam is tightly focused, the self-focusing is remarkable. Cross sections of the LISC are single fat ellipses. Since the decrease of the depth is much larger than that of the width, AR of the SiC grooves decreases with the increase of NA. Meanwhile, with the same set of laser parameters, a larger NA means a higher intensity of the laser irradiated on the SiC substrates. Therefore, more dangling bond appeared in the SiC lattice, accelerating diffusion of foreign matter species into the LISC. As a further consequence, deeper grooves were produced. Based on the above analysis, the 10× microscope objective with NA of 0.30 was employed to fabricate LISC with a single tapered cross-sectional shape.
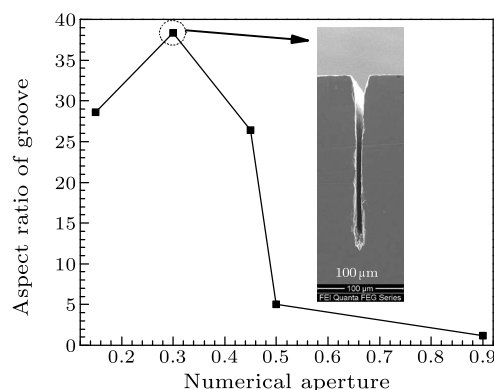

Fig. 2. AR of grooves versus NA.

To further understand the effects of laser average power on the grooves, a 10× microscope objective with NA of 0.3 was employed. The scanning velocity was set at 5 μm/s, while the laser average power was set from 5 to 40 mW with the increment of 5 mW. Figure 3 demonstrates the dependence of AR of the grooves on the laser average power, and the inset shows the morphology of the grooves produced with a laser average power of 40 mW. It is obvious that the AR of the grooves increases as the laser average power increases. For example, with the P of 5 mW, AR is 7; while it is 24 as P is 25 mW; with $P = 40$ mW, AR is 39. As mentioned above, multiphoton absorption associated with the extreme intensity of a femtosecond pulse is responsible for bond breaking and the subsequent creation of a dangling bond in SiC. As the incident laser average power increases, more laser energy could be absorbed by the material, resulting in the increase in the LISC depth. Meanwhile, the higher the incident laser average is, the larger the effective irradiation area on the SiC surface is. Consequently, the width and the entrance width of the LISC and the chemical etching produced grooves increase. Furthermore, due to the fact that the concentration of the femtosecond laser induced dangling bond increases with the increases in the laser average power, more foreign species of O would be trapped in the SiC substrate. As a result, the chemical and physical properties of the LISC are less stable as compared to those of the original one, which could accelerate the etching process. Therefore, the depth of LISC and the depth of the SiC grooves increase with an increase in the laser average power.
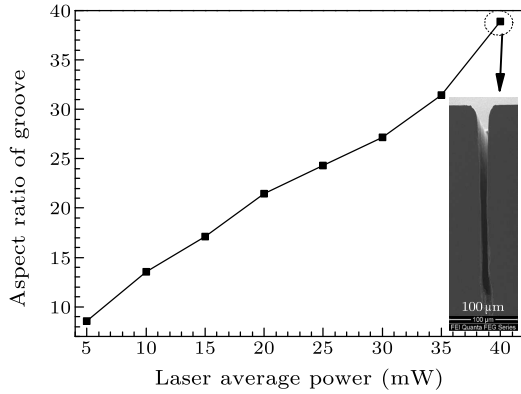
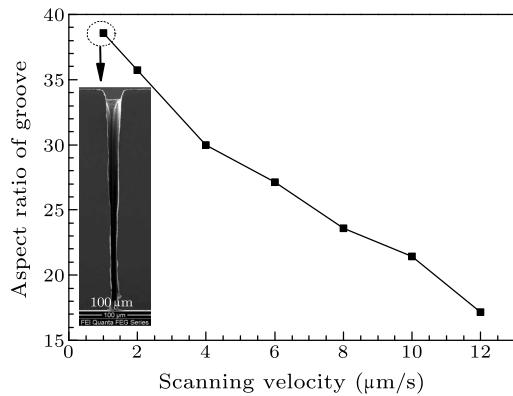**Fig. 3.** AR of grooves versus the laser average power.

Fig. 4. AR of grooves versus the laser scanning velocity.

Figure 4 illustrates the dependence of AR of the SiC grooves on the laser scanning velocity, and the inset shows the morphology of the grooves produced with a laser scanning velocity of 1 μm/s. The 10× microscope objective with NA of 0.3 was used. The laser average power was set at 30 mW. The scanning speeds were set to be 1, 2, 3, 4, 5, 6, 7, 8, 10, and 12 μm/s, respectively. It can be seen from Fig. 4 that the AR of the grooves decreases with the increase of the scanning speed. For example, with the scanning speed of 1 μm/s, AR is 37; while it is 30 as the scanning speed is 4 μm/s, and with scanning speed of 12 μm/s, AR is 17. This is due to the pulse accumulating effect. As the scanning velocity increases, the average pulses number on the unit area of the SiC samples decreases. This also means that the laser energy accumulated on the unit area of the SiC pattern decreases, resulting in the decrease of the depth of the LISC. While there is no significant change of the entrance width of the grooves, since the incident laser average power which decides the effective irradiation area on the pattern remains unchanged. As a result, the AR of the groove decreases with the increase of the scanning velocity.

The absorption spectrum of 6-H SiC was measured. Band gap of 6-H SiC is about 3.1 eV which corresponds to 400 nm photon energy. The material has a poor absorption at a wavelength larger than 400 nm. It shows strong absorption as the wavelength is smaller than 400 nm. Therefore, we believe that as long as the laser fluence is large enough to induce mul-

tiphoton absorption, it could be easy to obtain high-aspect-ratio grooves with the laser of a wavelength larger than 400 nm. In contrast, for the laser with a wavelength smaller than 400 nm, since the beam could not travel very long in the SiC due to the strong absorption, it is hard to obtain such high-aspect-ratio grooves.

In conclusion, we have proposed a simple method of fabricating high-aspect-ratio grooves in SiC using a femtosecond laser and chemical selective etching. Firstly, the LISC zones with aspect ratios up to 40 are induced on the SiC pattern. Then the grooves are produced as the LISC are removed by the chemical selective etching with a mixed solution of HF and HNO$_3$. The formation mechanism of the SiC grooves is attributed to the chemical reaction of the LISC with a mixed solution of HF and HNO$_3$. By using SEM equipped with EDS, the morphology and chemical composition of the SiC grooves are analyzed. It is observed that the sidewalls of the grooves are of a good quality. Furthermore, the effects of the numerical aperture of the microscope objective lens, the laser average power and the laser scanning velocity, on the AR of the grooves are systematically investigated, respectively. The AR of grooves increases with the increase of laser power. However, it decreases as the scanning speed increases. A microscope lens with a small NA should be chosen for higher AR grooves.

References

[1] Young D J et al 2004 *IEEE Sens. J.* **4** 464
[2] Östling M et al 2004 *Thin Solid Films* **469** 444
[3] Mehregany M and Zorman C A 1999 *Thin Solid Films* **355** 518
[4] Mehregany M et al 1998 *Proc. IEEE* **86** 1594
[5] Zorman C A, Rajgopal S, Fu X A, Jezeski R, Melzak J and Mehregany M 2002 *Electrochem. Solid-State Lett.* **5** G99
[6] Mehregany M et al 2000 *Int. Mater. Rev.* **45** 85
[7] Arbab A et al 1993 *Sens. Actuators* B **15** 19
[8] Morkoc H et al 1994 *J. Appl. Phys.* **76** 1363
[9] Sarro P M 2000 *Sens. Actuators* A **82** 210
[10] Xie K et al 1995 *Appl. Phys. Lett.* **67** 368
[11] Chabert P et al 2001 *Appl. Phys. Lett.* **79** 916
[12] Tanaka S et al 2001 *J. Vac. Sci. Technol.* B **19** 2173
[13] Khan F A et al 1999 *Appl. Phys. Lett.* **75** 2268
[14] Yih P H et al 1997 *Phys. Status Solidi* B **202** 605
[15] Pecholt B et al 2011 *J. Laser Appl.* **23** 012008
[16] Li C et al 2009 *Opt. Commun.* **282** 78
[17] Farsari M et al 2005 *J. Micromech. Microeng.* **15** 1786
[18] Xia X et al 2011 *Chin. Phys.* B **20** 044208
[19] Li B J et al 2012 *Acta Phys. Sin.* **61** 237901 (in Chinese)
[20] Jiang Y et al 2012 *Chin. Phys.* B **21** 064219
[21] Dong Y and Molian P 2003 *Appl. Phys.* A **77** 839
[22] Dong Y et al 2003 *J. Micromech. Microeng.* **13** 680
[23] Amera M S et al 2005 *Appl. Surf. Sci.* **242** 162
[24] Borowiec A and Haugen H K 2004 *Appl. Phys.* A **79** 521
[25] Khan F A et al 2001 *J. Electron. Mater.* **30** 212
[26] Kudrius T et al 2010 *J. Phys.* D **43** 145501
[27] Steinert M et al 2007 *J. Phys. Chem.* C **111** 2133
[28] Zhu J et al 2007 *Nanotechnology* **18** 365603
[29] Gattass et al 2008 *Nat. Photon.* **2** 219